EUROPEAN ORGANIZATION FOR NUCLEAR RESEARCH

CERN-PPE/95-118
July 24, 1995

Study of the $K^0_S K^0_S$ Final State in Two-Photon Collisions

The L3 Collaboration

Abstract

The reaction $e^+e^- \to e^+e^-\gamma^*\gamma^* \to e^+e^-K^0_S K^0_S$ is studied with the L3 detector at LEP and the formation of the $f_2'(1525)$ resonance is observed. For an integrated luminosity of 114 pb^{-1}, 31 ± 6 f_2' events are found. Their angular distribution is consistent with a pure helicity two. The radiative width times the branching ratio is measured to be $\Gamma_{\gamma\gamma}(f_2')\times Br(f_2' \to K\bar{K})=(0.093\pm\ 0.018\pm\ 0.022)$ keV. Only three events are found in the $f_2(1270)-a_2(1320)$ mass region, consistent with destructive f_2-a_2 interference in the $K^0_S K^0_S$ final state. The mixing angle of the tensor meson nonet is determined to be $\theta = (29.4^{+1.4}_{-1.6})^\circ$.

Submitted to *Phys. Lett. B*

1 Introduction

Electron-positron storage rings are widely used to investigate the behaviour of two-photon interactions via the process $e^+e^- \to e^+e^-\gamma^*\gamma^* \to e^+e^-X$, where γ^* is a virtual photon. The outgoing electron and positron carry nearly the full beam energy and their transverse momenta are usually so small that they are not detected (untagged event). This kind of event is characterized by an initial state $e^+e^-\gamma^*\gamma^*$, calculable by QED, and a low multiplicity final state. This process is particularly useful in the study of the properties of hadron resonances.

The total cross section σ_T of a resonance R is given by:

$$\sigma_T(e^+e^- \to e^+e^-R) = \int d^5\mathcal{L}_{\gamma\gamma}(\alpha_i) \cdot \sigma(\gamma^*\gamma^* \to R), \tag{1}$$

where $d^5\mathcal{L}_{\gamma\gamma}$ is the differential luminosity function giving the flux of virtual photons and $\alpha_i (i = 1, ..., 5)$ are the variables describing the scattered electron and positron. For quasi-real photons $\sigma(\gamma^*\gamma^* \to R)$ is given by the Breit-Wigner formula:

$$\sigma(\gamma^*\gamma^* \to R) = 8\pi(2J_R + 1)\frac{\Gamma_{\gamma\gamma}(R)\Gamma(R)}{(W_{\gamma\gamma}^2 - m_R^2)^2 + m_R^2\Gamma^2(R)}, \tag{2}$$

where $W_{\gamma\gamma}$ is the invariant mass of the two-photon system, m_R, J_R, $\Gamma_{\gamma\gamma}(R)$ and $\Gamma(R)$ are the mass, spin, two-photon partial width and total width of the resonance, respectively. Combining equations (1) and (2) leads to the proportionality relation

$$\sigma_T(e^+e^- \to e^+e^-R) = \mathcal{K} \cdot \Gamma_{\gamma\gamma}(R), \tag{3}$$

where the proportionality factor $\mathcal{K}$ can be evaluated by a Monte Carlo integration. Equation (3) is used to determine the two-photon partial width of the resonance.

The quantum numbers of the resonance must be compatible with the initial state of the two quasi-real photons. A neutral, unflavoured meson with even charge conjugation and helicity zero or two can be formed. In order to decay into $K_S^0K_S^0$, the resonance must have $(J)^{PC} = (\text{even})^{++}$.

For the 2^{++}, 1^3P_2 tensor meson nonet, the $f_2(1270)$, the $a_2^0(1320)$ and the $f_2'(1525)$ can be formed. However, since these three states are close in mass, interferences must be taken into account. According to SU(3), the $f_2(1270)$ interferes constructively with the $a_2^0(1320)$ in the K^+K^- final state but destructively in the $K^0\bar{K}^0$ final state [1]. Therefore, among the states of the tensor meson nonet, only the $f_2'(1525)$ is observable in the $K_S^0K_S^0$ final state as has been verified experimentally [2].

In this paper, we present an analysis of the reaction $e^+e^- \to e^+e^-K_S^0K_S^0$, where only the $K_S^0 \to \pi^+\pi^-$ decay is considered. The data correspond to an integrated luminosity of 114 pb^{-1} collected over the years 1991-94 by the L3 detector at LEP at center-of-mass energies around the Z resonance.

2 The L3 detector

The L3 experiment is described in detail in [3]. In this analysis, the charged particle tracker TEC (Time Expansion Chamber) is used mainly. The electromagnetic and hadronic calorimeters are used to veto photons.

The TEC is a cylindrical high resolution drift chamber with a sensitive region between 10 and 45 cm in the radial direction and a polar angle acceptance between 13° and 167°, in a

magnetic field of 0.5 T. There are 62 layers of wires with a spatial resolution of $\simeq$50 μm, giving a transverse momentum p_t resolution parametrized as $\sigma_{p_t}/p_t = 0.018p_t(\mathrm{GeV})\oplus 0.02$. The polar angle is measured by two layers of cylindrical Z-chambers surrounding the TEC, complemented by the measurement of charge division on the TEC wires. The azimuthal and polar angular resolutions are σ_φ =0.3 mrad and σ_θ =20 mrad, respectively. The latter is dominated by the interaction point spread σ_z $\simeq$10 mm. The interaction point is determined fill by fill using hadronic Z decays and has a r.m.s. width of σ_x =150 μm and σ_y =10 μm in the transverse plane, due to the beam size.

The electromagnetic calorimeter consists of an array of 10734 BGO crystals. The crystals are arranged in two half barrels with a polar angle coverage $42^\circ \leq \theta \leq 138^\circ$ and in two endcaps covering $11.6^\circ \leq \theta \leq 38^\circ$ and $142^\circ \leq \theta \leq 168.4^\circ$. A shower is defined with an energy threshold of 40 MeV.

The hadronic calorimeter (HCAL) consists of uranium absorbers and proportional wire chambers with a polar angle coverage $5^\circ \leq \theta \leq 175^\circ$.

The data for this analysis were collected using a charged-track trigger [4] with a low p_t threshold of 150 MeV. This trigger requires at least two charged tracks to be back-to-back in the plane transverse to the beam within $\pm 41^\circ$.

3 Event analysis

In order to select $e^+e^- \to e^+e^-\pi^+\pi^-\pi^+\pi^-$events, we require [5]:

- The total energy seen in the calorimeters must be smaller than 30 GeV to exclude annihilation events.
- There must be exactly four good charged tracks in the tracking chamber with a net charge of zero. A good track requires more than 20 hits out of a maximum of 62.
- The total momentum imbalance in the transverse plane must satisfy: $|\sum \overrightarrow{p_T}|^2 < 0.1$ GeV^2.
- Events with photons are rejected. A photon is defined as a shower in the electromagnetic calorimeter with an energy larger than 100 MeV. The signal must be present in more than two crystals, in order to reduce the noise contribution. The ratio between the energies deposited in the hadronic and electromagnetic calorimeters must be less than 0.2. There must be no charged track in a cone of 200 mrad around the photon direction.

24026 events are selected by these criteria, with an estimated background of 0.5% from other two-photon processes, evaluated by fitting the tail of the $|\sum \overrightarrow{p_T}|^2$ distribution. The beam-gas and beam-wall contributions are found to be negligible from inspection of the longitudinal vertex distribution.

The K^0_S's are identified by requiring a secondary vertex separated in the transverse plane by at least 1 mm from the primary interaction point. In order to select $K^0_S K^0_S$ exclusive events, we require:

- At least one of the two secondary vertices must be at a distance greater than 3 mm from the interaction point in the transverse plane.

- The angle between the flight direction of each K^0_S candidate (taken as the line between the interaction point and the secondary vertex in the transverse plane) and the total transverse momentum vector of the two outgoing tracks must be less than 0.6 rad.

- Since the two K^0_S's are produced back-to-back in the transverse plane, the angle between the flight directions of the two K^0_S candidates in this plane is required to be $\pi \pm 0.3$ rad.

- In order to suppress low energy photon conversions, the mass of the two oppositely charged particles forming each secondary vertex must be greater than 150 MeV.

- The invariant masses of the two K^0_S candidates must be within ± 25 MeV of the K^0_S mass. Figure 1 shows the $\pi^+\pi^-$ mass distribution with a 3 mm vertex cut for the K^0_S. Fitting this distribution, we find a mass resolution of $\sigma = 9.6 \pm 0.8$ MeV, consistent with the Monte Carlo simulation.

With these selection criteria, 62 events are found in the data sample. In order to improve the precision on the $K^0_SK^0_S$ invariant mass, a kinematical fit is performed on each $K^0_S \to \pi^+\pi^-$ decay. The resulting $K^0_SK^0_S$ invariant mass spectrum is shown in Figure 2. The spectrum is dominated by the $f_2'(1525)$ resonance: 35 events are in the mass region $1420 \leq M_{K^0_SK^0_S} \leq 1660$ MeV. Only three events are found in the $f_2(1270)-a_2^0(1320)$ mass region: this is consistent with the theoretical prediction [1] of destructive $f_2-a_2^0$ interference in the $K^0_SK^0_S$ final state. 19 events are found in the mass region around 1800 MeV ($1720 \leq M_{K^0_SK^0_S} \leq 1930$ MeV).

The background due to misidentified K^0_S pairs is estimated by a study of the K^0_S sidebands: one K^0_S is taken within $\pm$ 25 MeV from the K^0_S mass and the other in the two sidebands of 25 MeV just outside the K^0_S region. Three events are found in the $f_2'(1525)$ mass region and two in the 1800 MeV mass region. The background due to the $K^0_SK^\pm\pi^\mp$ final state is determined to be negligible by a Monte Carlo simulation.

A maximum likelihood fit using two Gaussians and a flat background is then performed on the $K^0_SK^0_S$ mass spectrum. All the parameters are left free while the normalization is fixed by the total number of events. The fit is shown in Figure 2 and the results are summarized in Table 1.

	First peak $f_2'(1525)$	Second peak
Mass (MeV)	1529 ± 10	1793 ± 18
Sigma (MeV)	48 ± 8	51 ± 19
Number of events	31.1 ± 6.3	15.0 ± 5.1

Table 1: Results from the maximum likelihood fit of the $K^0_SK^0_S$ invariant mass spectrum.

While the $f_2'(1525)$ statistical significance is five standard deviations, the statistical significance of the second peak is 2.9 standard deviations, thus requiring more statistics to investigate the nature of this peak.

The measured width for the $f_2'(1525)$ is consistent with the Monte Carlo simulation. If we use the Monte Carlo resolution for a zero-width resonance and unfold the Breit-Wigner distribution, a value of $\Gamma(f_2'(1525)) = (76 \pm 40)$MeV is obtained, consistent with the PDG value [6].

In order to correct the data for the detector acceptance and efficiency, a Monte Carlo procedure is used [7]. The nominal $f_2'(1525)$ parameters [6] are used for the generation. The

angular distribution of the two K^0_S's in the two-photon center-of-mass system is generated according to phase space i.e. uniform in $\cos\theta^*$ and in ϕ^*, where θ^* and ϕ^* are the polar and azimuthal angles taking the z direction parallel to the electron beam. In order to take into account the helicity of a spin-two resonance, a weight is assigned to each generated event according to the weight functions [8]: $w = (\cos^2\theta^* - \frac{1}{3})^2$ for the helicity-zero contribution and $w = \sin^4\theta^*$ for the helicity-two contribution.

All the events are passed through the full detector simulation program and are reconstructed following the same procedure used for the data. Although the detector acceptance is rather high (15% for helicity zero and 30% for helicity two), the trigger efficiency (83%), the data selection (72%) and the analysis cuts ($\sim$ 30%) give a total efficiency of 1.9% for helicity zero and 4.1% for helicity two.

4 Results

The total cross section σ_T times the branching ratio Br into $K\bar{K}$ is measured using the formula

$$\sigma_T \times \mathrm{Br} = \frac{N_{obs} - N_{back}}{\mathcal{L}\varepsilon}, \tag{4}$$

where $\mathcal{L}$ is the integrated luminosity [9] and ε is the total efficiency. The number of signal events $N_{obs} - N_{back}$ is determined from the maximum likelihood fit (Table 1). From our data only $\sigma_T \times \mathrm{Br}(f'_2 \to K^0_S K^0_S \to \pi^+\pi^-\pi^+\pi^-)$ can be measured. Using the PDG [6] value for $\mathrm{Br}(K^0_S \to \pi^+\pi^-)$ and $\mathrm{Br}(f'_2 \to K\bar{K}) = 4 \times \mathrm{Br}(f'_2 \to K^0_S K^0_S)$ from isospin conservation, we determine $\sigma_T \times \mathrm{Br}(f'_2 \to K\bar{K})$. The results are reported in Table 2 for a pure helicity-zero or helicity-two hypothesis. The difference between the two helicity results shows clearly the importance of taking the angular distribution into account.

$\sigma_T \times \mathrm{Br}(f'_2 \to K\bar{K})$ (pb)	
Helicity 0	Helicity 2
$120 \pm 24 \pm 29$	$56 \pm 11 \pm 13$

Table 2: The measurement of the cross section times the branching ratio for the $f'_2(1525)$ for the two possible helicity states. The first error is statistical and the second is systematic.

The contributions to the systematic error on $\sigma_T \times \mathrm{Br}$ due to the selection efficiency (16%) and the kinematic cuts (13%) are evaluated using the Monte Carlo simulation and by performing cut variations. The uncertainty in the trigger efficiency is estimated to be 11%. The contribution due to the maximum likelihood fit procedure is estimated to be 6% and is evaluated by changing the background parametrization and the fitted mass region. The total systematic error on $\sigma_T \times \mathrm{Br}$ for the f'_2 is found to be 24%.

A study of the angular distribution of the two K^0_S's from f'_2 decay in the two-photon center of mass is performed. The total efficiency as a function of the polar angle θ^* is shown in Figure 3. The experimental polar angle distribution is compared with the Monte Carlo in Figure 4 for both the helicity-zero and helicity-two cases. The Monte Carlo distributions are normalized to the same number of events as in the data and no background subtraction is done. The χ^2 values for the helicity zero and helicity two hypotheses are 23 and 10 for eight degrees of

freedom respectively, thus preferring the helicity two. This is in agreement with the theoretical predictions that the helicity-two contribution should dominate [10].

The product $\Gamma_{\gamma\gamma}(f_2')\times$ Br$(f_2' \to K\bar{K})$ is measured using the formula

$$\Gamma_{\gamma\gamma}(f_2') \times \mathrm{Br}(f_2' \to K\bar{K}) = \frac{\sigma_T \times \mathrm{Br}(f_2' \to K\bar{K})}{\mathcal{K}}, \tag{5}$$

where the proportionality factor $\mathcal{K}$ is evaluated by Monte Carlo integration. The results for the measured $\Gamma_{\gamma\gamma}(f_2')\times$Br$(f_2' \to K\bar{K})$ are reported in Table 3 for the hypotheses of a pure helicity-zero and helicity-two contribution to the cross section.

$\Gamma_{\gamma\gamma}(f_2')\times$ Br$(f_2' \to K\bar{K})$ (keV)	
Helicity 0	Helicity 2
$0.198 \pm 0.040 \pm 0.050$	$0.093 \pm 0.018 \pm 0.022$

Table 3: The measurement of $\Gamma_{\gamma\gamma}(f_2')\times$Br$(f_2' \to K\bar{K})$ for the two possible helicity states. The first error is statistical and the second is systematic.

From the measurement of the radiative width of the $f_2'(1525)$, it is possible to determine the mixing angle θ between the singlet and the octet members of the tensor meson nonet. Using the relation [11]

$$\Gamma_{\gamma\gamma}(R) = \frac{g_{T\gamma\gamma}^2}{4\pi}\frac{m_R^3}{80\mu^2}, \tag{6}$$

where μ is a constant of the nonet and $g_{T\gamma\gamma}$ is the two-photon coupling of the resonance, proportional to the square of the quark charges, the following relation is derived [8]:

$$\frac{\Gamma_{\gamma\gamma}(f_2')}{\Gamma_{\gamma\gamma}(f_2)} = \frac{m^3_{f_2'(1525)}}{m^3_{f_2(1270)}} \cdot \frac{(\cos\theta - 2\sqrt{2}\sin\theta)^2}{(\sin\theta + 2\sqrt{2}\cos\theta)^2}. \tag{7}$$

Using the result of the present analysis and the PDG values [6] for Br$(f_2' \to K\bar{K}) = (71.2^{+2.0}_{-2.5})\%$ and $\Gamma_{\gamma\gamma}(f_2) = (2.4 \pm 0.3)$ keV, a value of

$$\theta = (29.4^{+1.4}_{-1.6})^\circ$$

is obtained under the hypothesis of helicity two for the $f_2'(1525)$. The result indicates a deviation from ideal mixing ($\theta = 35.3^\circ$) and is in agreement with the value of $\theta = (28 \pm 3)^\circ$ [8] found from the Gell-Mann$-$Okubo mass formula [12]. Our result is also in agreement with the value of $\theta = (28 \pm 2)^\circ$ found in a recent analysis of the tensor nonet [13].

If not due to a statistical fluctuation, the peak near 1800 MeV could be the formation of a resonance belonging to an $(\mathrm{even})^{++}$ meson nonet.

5 Conclusions

The reaction $e^+e^- \to e^+e^-\gamma^*\gamma^* \to e^+e^-K^0_SK^0_S$ is studied with the L3 detector at LEP. From an integrated luminosity of 114 pb^{-1}, 31 ± 6 $f_2'(1525)$ events are found. The angular distribution is consistent with a pure helicity-two state. We obtain

$$\Gamma_{\gamma\gamma}(f_2') \times \mathrm{Br}(f_2' \to K\bar{K}) = (0.093 \pm 0.018 \pm 0.022) \text{ keV}$$

under the hypothesis of pure helicity two. This value is consistent with previous measurements [2, 14].

Only three events are found in the $f_2(1270)$–$a_2(1320)$ mass region, consistent with the theoretical prediction [1] of destructive f_2-a_2 interference in the $K^0_SK^0_S$ final state.

The $K^0_SK^0_S$ mass spectrum shows an enhancement near 1800 MeV with a statistical significance of 2.9 standard deviations.

The mixing angle between the singlet and octet members of the SU(3) tensor meson nonet is evaluated to be $\theta = (29.4^{+1.4}_{-1.6})^\circ$.

6 Acknowledgments

We wish to express our gratitude to the CERN accelerator divisions for the excellent performance of the LEP machine. We acknowledge the contributions of all the engineers and technicians who have participated in the construction and maintenance of this experiment. Those of us who are not from member states thank CERN for its hospitality and help.

The L3 Collaboration:

M.Acciarri,[27] A.Adam,[45] O.Adriani,[17] M.Aguilar-Benitez,[26] S.Ahlen,[11] B.Alpat,[34] J.Alcaraz,[26] J.Allaby,[18] A.Aloisio,[29] G.Alverson,[12] M.G.Alviggi,[29] G.Ambrosi,[34] Q.An,[19] H.Anderhub,[48] V.P.Andreev,[38] T.Angelescu,[13] D.Antreasyan,[9] A.Arefiev,[28] T.Azemoon,[3] T.Aziz,[10] P.V.K.S.Baba,[19] P.Bagnaia,[37,18] L.Baksay,[43] R.C.Ball,[3] S.Banerjee,[10] K.Banicz,[45] R.Barillère,[18] L.Barone,[37] P.Bartalini,[34] A.Baschirotto,[27] M.Basile,[9] R.Battiston,[34] A.Bay,[23] F.Becattini,[17] U.Becker,[16] F.Behner,[48] Gy.L.Bencze,[14] J.Berdugo,[26] P.Berges,[16] B.Bertucci,[18] B.L.Betev,[48] M.Biasini,[34] A.Biland,[48] G.M.Bilei[34] R.Bizzarri,[37] J.J.Blaising,[18] G.J.Bobbink,[2] R.Bock,[1] A.Böhm,[1] B.Borgia,[37] A.Boucham,[4] D.Bourilkov,[48] M.Bourquin,[20] D.Boutigny,[4] S.Braccini,[17] E.Brambilla,[16] J.G.Branson,[39] V.Brigljevic,[48] I.C.Brock,[35] A.Buijs,[44] A.Bujak,[45] J.D.Burger,[16] W.J.Burger,[20] C.Burgos,[26] J.Busenitz,[43] A.Buytenhuijs,[31] X.D.Cai,[19] M.Capell,[16] G.Cara Romeo,[9] M.Caria,[34] G.Carlino,[29] A.M.Cartacci,[17] J.Casaus,[26] G.Castellini,[17] R.Castello,[27] F.Cavallari,[37] N.Cavallo,[29] C.Cecchi,[20] M.Cerrada,[26] F.Cesaroni,[37] M.Chamizo,[26] A.Chan,[50] Y.H.Chang,[50] U.K.Chaturvedi,[19] M.Chemarin,[25] A.Chen,[50] C.Chen,[7] G.Chen,[7] G.M.Chen,[7] H.F.Chen,[21] H.S.Chen,[7] M.Chen,[16] G.Chiefari,[29] C.Y.Chien,[5] M.T.Choi,[42] L.Cifarelli,[9] F.Cindolo,[9] C.Civinini,[17] I.Clare,[16] R.Clare,[16] T.E.Coan,[24] H.O.Cohn,[32] G.Coignet,[4] A.P.Colijn,[2] N.Colino,[18] V.Commichau,[1] S.Costantini,[37] F.Cotorobai,[13] B.de la Cruz,[26] X.T.Cui,[19] X.Y.Cui,[19] T.S.Dai,[16] R.D'Alessandro,[17] R.de Asmundis,[29] H.De Boeck,[31] A.Degré,[4] K.Deiters,[46] E.Dénes,[14] P.Denes,[36] F.DeNotaristefani,[37] D.DiBitonto,[43] M.Diemoz,[37] D.van Dierendonck,[2] F.Di Lodovico,[37] C.Dionisi,[37] M.Dittmar,[48] A.Dominguez,[39] A.Doria,[29] I.Dorne,[4] M.T.Dova,[19,♯] E.Drago,[29] D.Duchesneau,[18] P.Duinker,[2] I.Duran,[40] S.Dutta,[10] S.Easo,[34] Yu.Efremenko,[32] H.El Mamouni,[25] A.Engler,[35] F.J.Eppling,[16] F.C.Erné,[2] J.P.Ernenwein,[25] P.Extermann,[20] R.Fabbretti,[46] M.Fabre,[46] R.Faccini,[37] S.Falciano,[37] A.Favara,[17] J.Fay,[25] M.Felcini,[48] T.Ferguson,[35] D.Fernandez,[26] G.Fernandez,[26] F.Ferroni,[37] H.Fesefeldt,[1] E.Fiandrini,[34] J.H.Field,[20] F.Filthaut,[35] P.H.Fisher,[16] G.Forconi,[16] L.Fredj,[20] K.Freudenreich,[48] M.Gailloud,[23] Yu.Galaktionov,[28,16] S.N.Ganguli,[10] P.Garcia-Abia,[26] S.S.Gau,[12] S.Gentile,[37] J.Gerald,[5] N.Gheordanescu,[13] S.Giagu,[37] S.Goldfarb,[23] J.Goldstein,[11] Z.F.Gong,[21] E.Gonzalez,[26] A.Gougas,[5] D.Goujon,[20] G.Gratta,[33] M.W.Gruenewald,[8] C.Gu,[19] M.Guanziroli,[19] V.K.Gupta,[36] A.Gurtu,[10] H.R.Gustafson,[3] L.J.Gutay,[45] B.Hartmann,[1] A.Hasan,[30] J.T.He,[7] T.Hebbeker,[8] A.Hervé,[18] K.Hilgers,[1] W.C.van Hoek,[31] H.Hofer,[48] H.Hoorani,[20] S.R.Hou,[50] G.Hu,[19] M.M.Ilyas,[19] V.Innocente,[18] H.Janssen,[4] B.N.Jin,[7] L.W.Jones,[3] P.de Jong,[16] I.Josa-Mutuberria,[26] A.Kasser,[23] R.A.Khan,[19] Yu.Kamyshkov,[32] P.Kapinos,[47] J.S.Kapustinsky,[24] Y.Karyotakis,[4] M.Kaur,[19] S.Khokhar,[19] M.N.Kienzle-Focacci,[20] D.Kim,[5] J.K.Kim,[42] S.C.Kim,[42] Y.G.Kim,[42] W.W.Kinnison,[24] A.Kirkby,[33] D.Kirkby,[33] J.Kirkby,[18] W.Kittel,[31] A.Klimentov,[16,28] A.C.König,[31] E.Koffeman,[2] O.Kornadt,[1] V.Koutsenko,[16,28] A.Koulbardis,[38] R.W.Kraemer,[35] T.Kramer,[16] W.Krenz,[1] H.Kuijten,[31] A.Kunin,[16,28] P.Ladron de Guevara,[26] G.Landi,[17] C.Lapoint,[16] K.Lassila-Perini,[48] P.Laurikainen,[22] M.Lebeau,[18] A.Lebedev,[16] P.Lebrun,[25] P.Lecomte,[48] P.Lecoq,[18] P.Le Coultre,[48] J.S.Lee,[42] K.Y.Lee,[42] C.Leggett,[3] J.M.Le Goff,[18] R.Leiste,[47] M.Lenti,[17] E.Leonardi,[37] P.Levtchenko,[38] C.Li,[21,19] E.Lieb,[47] W.T.Lin,[50] F.L.Linde,[2] B.Lindemann,[1] L.Lista,[29] Y.Liu,[19] Z.A.Liu,[7] W.Lohmann,[47] E.Longo,[37] W.Lu,[33] Y.S.Lu,[7] K.Lübelsmeyer,[1] C.Luci,[37] D.Luckey,[16] L.Ludovici,[37] L.Luminari,[37] W.Lustermann,[46] W.G.Ma,[21] A.Macchiolo,[17] M.Maity,[10] L.Malgeri,[37] R.Malik,[19] A.Malinin,[28] C.Maña,[26] S.Mangla,[10] M.Maolinbay,[48] P.Marchesini,[48] A.Marin,[11] J.P.Martin,[25] F.Marzano,[37] G.G.G.Massaro,[2] K.Mazumdar,[10] D.McNally,[18] S.Mele,[29] L.Merola,[29] M.Meschini,[17] W.J.Metzger,[31] Y.Mi,[23] A.Mihul,[13] A.J.W.van Mil,[31] Y.Mir,[19] G.Mirabelli,[37] J.Mnich,[18] M.Möller,[1] B.Monteleoni,[17] R.Moore,[3] R.Morand,[4] S.Morganti,[37] N.E.Moulai,[19] R.Mount,[33] S.Müller,[1] F.Muheim,[20] E.Nagy,[14] S.Nahn,[16] M.Napolitano,[29] F.Nessi-Tedaldi,[48] H.Newman,[33] M.A.Niaz,[19] A.Nippe,[1] H.Nowak,[47] G.Organtini,[37] R.Ostonen,[22] D.Pandoulas,[1] S.Paoletti,[37] P.Paolucci,[29] G.Pascale,[37] G.Passaleva,[17] S.Patricelli,[29] T.Paul,[34] M.Pauluzzi,[34] C.Paus,[1] F.Pauss,[48] Y.J.Pei,[1] S.Pensotti,[27] D.Perret-Gallix,[4] S.Petrak,[8] A.Pevsner,[5] D.Piccolo,[29] M.Pieri,[17] J.C.Pinto,[35] P.A.Piroué,[36] E.Pistolesi,[17] V.Plyaskin,[28] M.Pohl,[48] V.Pojidaev,[28,17] H.Postema,[16] N.Produit,[20] K.N.Qureshi,[19] R.Raghavan,[10] G.Rahal-Callot,[48] P.G.Rancoita,[27] M.Rattaggi,[27] G.Raven,[39] P.Razis,[30] K.Read,[32] M.Redaelli,[27] D.Ren,[48] Z.Ren,[19] M.Rescigno,[37] S.Reucroft,[12] A.Ricker,[1] S.Riemann,[47] B.C.Riemers,[45] K.Riles,[3] O.Rind,[3] H.A.Rizvi,[19] S.Ro,[42] A.Robohm,[48] J.Rodin,[16] F.J.Rodriguez,[26] B.P.Roe,[3] M.Röhner,[1] S.Röhner,[1] L.Romero,[26] S.Rosier-Lees,[4] Ph.Rosselet,[23] W.van Rossum,[44] S.Roth,[1] J.A.Rubio,[18] H.Rykaczewski,[48] J.Salicio,[18] J.M.Salicio,[26] E.Sanchez,[26] A.Santocchia,[34] M.E.Sarakinos,[22] S.Sarkar,[10] G.Sartorelli,[19] M.Sassowsky,[1] G.Sauvage,[4] C.Schäfer,[1] V.Schegelsky,[38] D.Schmitz,[1] P.Schmitz,[1] M.Schneegans,[4] B.Schoeneich,[47] N.Scholz,[48] H.Schopper,[49] D.J.Schotanus,[31] R.Schulte,[1] K.Schultze,[1] J.Schwenke,[1] G.Schwering,[1] C.Sciacca,[29] R.Sehgal,[19] P.G.Seiler,[46] J.C.Sens,[50] L.Servoli,[34] S.Shevchenko,[33] N.Shivarov,[41] V.Shoutko,[28] J.Shukla,[24] E.Shumilov,[28] D.Son,[42] A.Sopczak,[18] V.Soulimov,[29] B.Smith,[16] T.Spickermann,[1] P.Spillantini,[17] M.Steuer,[16] D.P.Stickland,[36] F.Sticozzi,[16] H.Stone,[36] B.Stoyanov,[41] K.Strauch,[15] K.Sudhakar,[10] G.Sultanov,[19] L.Z.Sun,[21,19] G.F.Susinno,[20] H.Suter,[48] J.D.Swain,[19] X.W.Tang,[7] L.Tauscher,[6] L.Taylor,[12] R.Timellini,[9] Samuel C.C.Ting,[16] S.M.Ting,[16] O.Toker,[34] F.Tonisch,[47] M.Tonutti,[1] S.C.Tonwar,[10] J.Tóth,[14] A.Tsaregorodtsev,[38] G.Tsipolitis,[35] C.Tully,[36] H.Tuchscherer,[43] J.Ulbricht,[48] L.Urbán,[14] U.Uwer,[1] E.Valente,[37] R.T.Van de Walle,[31] I.Vetlitsky,[28] G.Viertel,[48] P.Vikas,[19] U.Vikas,[19] M.Vivargent,[4] R.Völkert,[47] H.Vogel,[35] H.Vogt,[47] I.Vorobiev,[28] A.A.Vorobyov,[38] An.A.Vorobyov,[38] L.Vuilleumier,[23] M.Wadhwa,[6] W.Wallraff,[1] J.C.Wang,[16] X.L.Wang,[21] Y.F.Wang,[16] Z.M.Wang,[19,21] A.Weber,[1] R.Weill,[23] C.Willmott,[26] F.Wittgenstein,[18] S.X.Wu,[19] S.Wynhoff,[1] J.Xu,[11] Z.Z.Xu,[21] B.Z.Yang,[21] C.G.Yang,[7] G.Yang,[19] X.Y.Yao,[7] C.H.Ye,[19] J.B.Ye,[21] Q.Ye,[19] S.C.Yeh,[50] J.M.You,[35] N.Yunus,[19] C.Zaccardelli,[33] An.Zalite,[38] P.Zemp,[48] J.Y.Zeng,[7] M.Zeng,[19] Y.Zeng,[1] Z.Zhang,[7] Z.P.Zhang,[21,19] B.Zhou,[11] G.J.Zhou,[7] J.F.Zhou,[1] Y.Zhou,[3] G.Y.Zhu,[7] R.Y.Zhu,[33] A.Zichichi,[9,18,19] B.C.C.van der Zwaan.[2]

1 I. Physikalisches Institut, RWTH, D-52056 Aachen, FRG[§]
III. Physikalisches Institut, RWTH, D-52056 Aachen, FRG[§]
2 National Institute for High Energy Physics, NIKHEF, and University of Amsterdam, NL-1009 DB Amsterdam, The Netherlands
3 University of Michigan, Ann Arbor, MI 48109, USA
4 Laboratoire d'Annecy-le-Vieux de Physique des Particules, LAPP,IN2P3-CNRS, BP 110, F-74941 Annecy-le-Vieux CEDEX, France
5 Johns Hopkins University, Baltimore, MD 21218, USA
6 Institute of Physics, University of Basel, CH-4056 Basel, Switzerland
7 Institute of High Energy Physics, IHEP, 100039 Beijing, China
8 Humboldt University, D-10099 Berlin, FRG[§]
9 INFN-Sezione di Bologna, I-40126 Bologna, Italy
10 Tata Institute of Fundamental Research, Bombay 400 005, India
11 Boston University, Boston, MA 02215, USA
12 Northeastern University, Boston, MA 02115, USA
13 Institute of Atomic Physics and University of Bucharest, R-76900 Bucharest, Romania
14 Central Research Institute for Physics of the Hungarian Academy of Sciences, H-1525 Budapest 114, Hungary[‡]
15 Harvard University, Cambridge, MA 02139, USA
16 Massachusetts Institute of Technology, Cambridge, MA 02139, USA
17 INFN Sezione di Firenze and University of Florence, I-50125 Florence, Italy
18 European Laboratory for Particle Physics, CERN, CH-1211 Geneva 23, Switzerland
19 World Laboratory, FBLJA Project, CH-1211 Geneva 23, Switzerland
20 University of Geneva, CH-1211 Geneva 4, Switzerland
21 Chinese University of Science and Technology, USTC, Hefei, Anhui 230 029, China
22 SEFT, Research Institute for High Energy Physics, P.O. Box 9, SF-00014 Helsinki, Finland
23 University of Lausanne, CH-1015 Lausanne, Switzerland
24 Los Alamos National Laboratory, Los Alamos, NM 87544, USA
25 Institut de Physique Nucléaire de Lyon, IN2P3-CNRS,Université Claude Bernard, F-69622 Villeurbanne Cedex, France
26 Centro de Investigaciones Energeticas, Medioambientales y Tecnologicas, CIEMAT, E-28040 Madrid, Spain[♭]
27 INFN-Sezione di Milano, I-20133 Milan, Italy
28 Institute of Theoretical and Experimental Physics, ITEP, Moscow, Russia
29 INFN-Sezione di Napoli and University of Naples, I-80125 Naples, Italy
30 Department of Natural Sciences, University of Cyprus, Nicosia, Cyprus
31 University of Nymegen and NIKHEF, NL-6525 ED Nymegen, The Netherlands
32 Oak Ridge National Laboratory, Oak Ridge, TN 37831, USA
33 California Institute of Technology, Pasadena, CA 91125, USA
34 INFN-Sezione di Perugia and Universitá Degli Studi di Perugia, I-06100 Perugia, Italy
35 Carnegie Mellon University, Pittsburgh, PA 15213, USA
36 Princeton University, Princeton, NJ 08544, USA
37 INFN-Sezione di Roma and University of Rome, "La Sapienza", I-00185 Rome, Italy
38 Nuclear Physics Institute, St. Petersburg, Russia
39 University of California, San Diego, CA 92093, USA
40 Dept. de Fisica de Particulas Elementales, Univ. de Santiago, E-15706 Santiago de Compostela, Spain
41 Bulgarian Academy of Sciences, Central Laboratory of Mechatronics and Instrumentation, BU-1113 Sofia, Bulgaria
42 Center for High Energy Physics, Korea Advanced Inst. of Sciences and Technology, 305-701 Taejon, Republic of Korea
43 University of Alabama, Tuscaloosa, AL 35486, USA
44 Utrecht University and NIKHEF, NL-3584 CB Utrecht, The Netherlands
45 Purdue University, West Lafayette, IN 47907, USA
46 Paul Scherrer Institut, PSI, CH-5232 Villigen, Switzerland
47 DESY-Institut für Hochenergiephysik, D-15738 Zeuthen, FRG
48 Eidgenössische Technische Hochschule, ETH Zürich, CH-8093 Zürich, Switzerland
49 University of Hamburg, D-22761 Hamburg, FRG
50 High Energy Physics Group, Taiwan, China
§ Supported by the German Bundesministerium für Bildung, Wissenschaft, Forschung und Technologie
‡ Supported by the Hungarian OTKA fund under contract numbers 2970 and T14459.
♭ Supported also by the Comisión Interministerial de Ciencia y Tecnología
♯ Also supported by CONICET and Universidad Nacional de La Plata, CC 67, 1900 La Plata, Argentina

References

[1] H. J. Lipkin, Nucl. Phys. **B 7** (1968) 321; Procs. EPS Int. Conf. on High Energy Physics, Palermo 1975, p. 609;
D. Faiman et al., Phys. Lett. **59 B** (1975) 269.

[2] TASSO Collab., M. Althoff et al., Phys. Lett. **121 B** (1982) 216;
TASSO Collab., M. Althoff et al., Z. Phys. **C 29** (1985) 189;
PLUTO Collab., C. Berger et al., Z. Phys. **C 37** (1988) 329;
CELLO Collab., H. J. Behrend et al., Z. Phys. **C 43** (1989) 91.

[3] L3 Collab., B. Adeva et al., Nucl. Inst. Meth. **A 289** (1990) 35;
L3 Collab., O. Adriani et al., Phys. Rep. **236** (1993) 1.

[4] P. Béné et al., Nucl. Inst. Meth. **A 306** (1991) 150;
Y. Bertsh et al., Nucl. Inst. Meth. **A 340** (1993) 309 and 322;
C. Dionisi et al., Nucl. Inst. Meth. **A 336** (1993) 78.

[5] S. Braccini, "Studio delle interazioni fotone-fotone con il rivelatore L3 al LEP", Tesi di Laurea, University of Florence, Italy (1995).

[6] Particle Data Group, L. Montanet et al., Review of Particle Properties, Phys. Rev. **D 50** (1994) 1.

[7] F. L. Linde, "Charm Production in Two-Photon Collisions", Ph. D. Thesis, Rijksuniversiteit Leiden, (1988).

[8] H. Kolanoski, "Two-Photon Physics at e^+e^- Storage Rings", Springer-Verlag, 1984.

[9] L3 Collab., M. Acciarri et al., Z. Phys. **C62** (1994) 551.

[10] B. Schrempp-Otto et al., Phys. Lett. **36 B** (1971) 463;
G. Köpp et al., Nucl. Phys. **B 70** (1974) 461;
P. Grassberger and R. Kögerler, Nucl. Phys. **B 106** (1976) 451.

[11] P. Singer, Phys. Lett. **124 B** (1983) 531.

[12] M. Gell-Mann, Phys. Rev. **125** (1962) 1067;
S. Okubo, Prog. Theor. Phys. **27** (1962) 949.

[13] K. Peters and E. Klempt, Phys. Lett. **352 B** (1995) 467.

[14] ARGUS Collab., H. Albrecht et al., Z. Phys. **C 48** (1990) 183.

Figure Captions

Figure 1 : The $\pi^+\pi^-$ mass spectrum for reconstructed secondary vertices which are more than 3 mm from the interaction point. The curve is the result of a fit using a third-order polynomial for the background and a Gaussian for the peak. The arrows indicate the signal region.

Figure 2 : The $K^0_S K^0_S$ invariant mass spectrum: the solid line corresponds to the maximum likelihood fit. The background is fitted by a constant (dashed line) and the two peaks by Gaussian curves.

Figure 3 : The total detection efficiency for $K^0_S K^0_S$ events as a function of $|\cos\theta^*|$. The error bars are due to Monte Carlo statistics.

Figure 4 : The $K^0_S K^0_S$ polar angular distribution compared with the Monte Carlo distributions for the hypothesis of a pure helicity-zero (dash-dotted curve) and helicity-two (solid curve) contribution to the cross section for the $f'_2(1525)$. The Monte Carlo curves are normalized to the same number of events as the data.

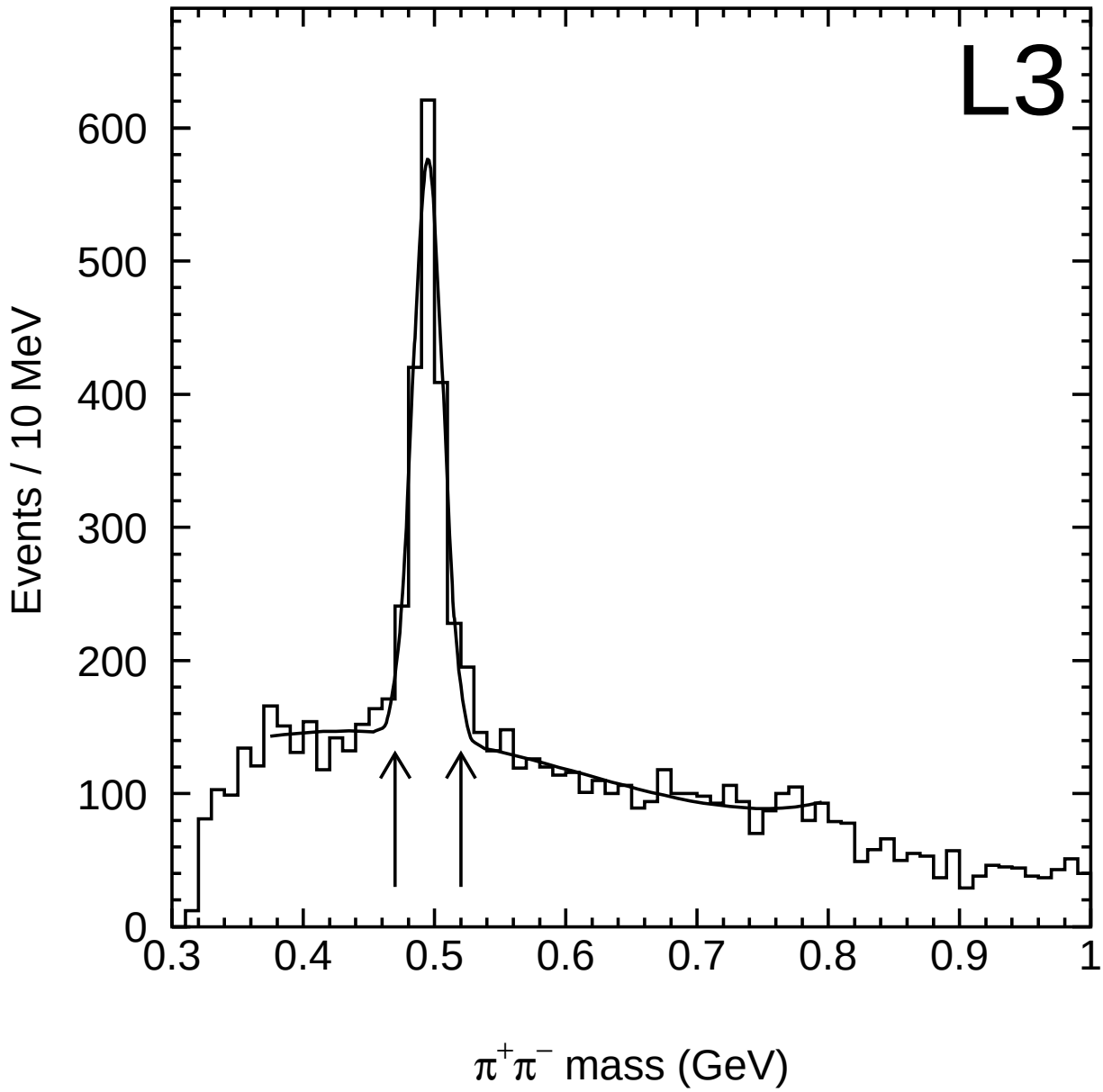
L3
Events / 10 MeV
600
500
400
300
200
100
0
0.3
0.4
0.5
0.6
0.7
0.8
0.9
1
$\pi^+\pi^-$ mass (GeV)

Figure 1

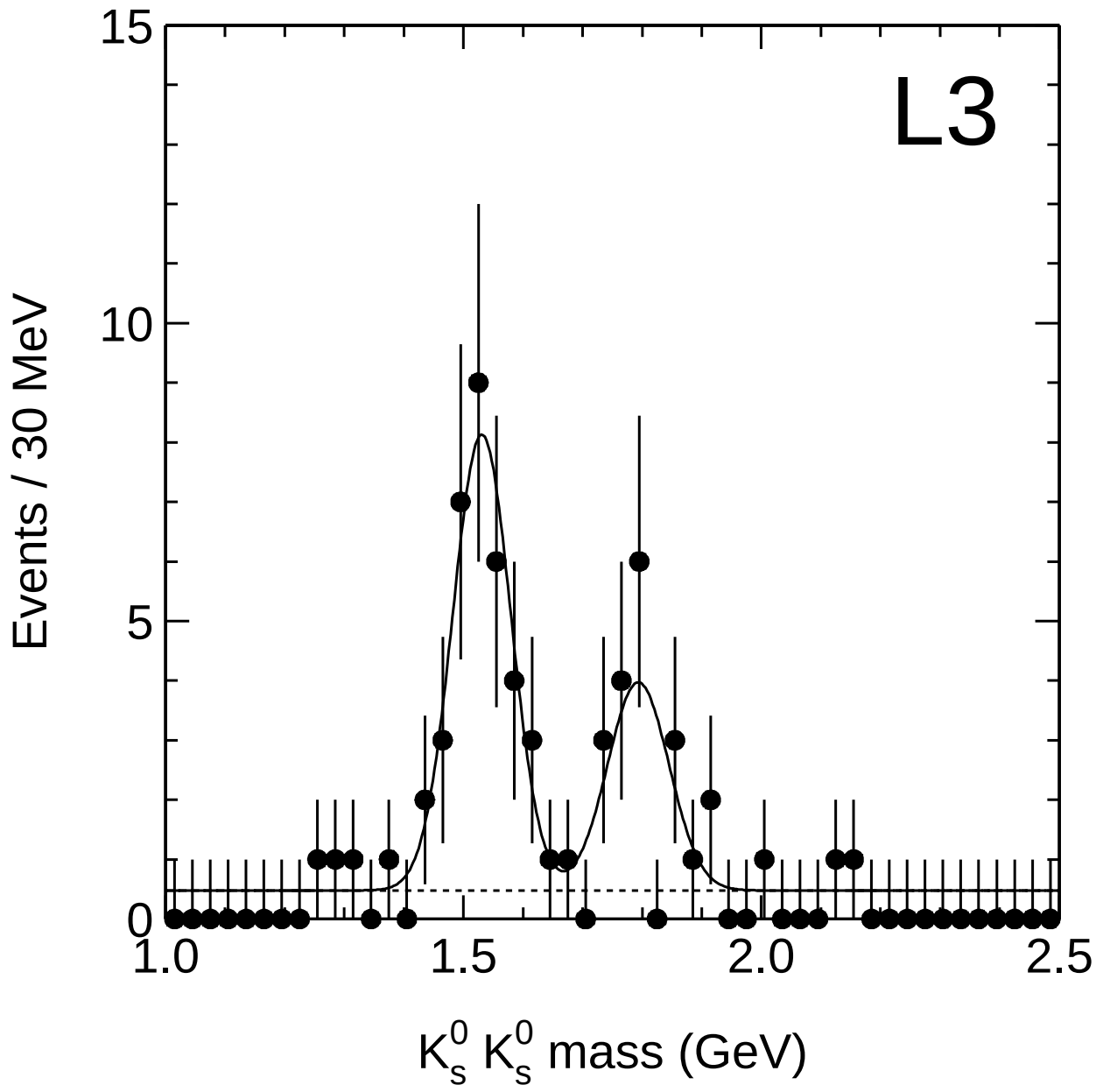

Figure 2

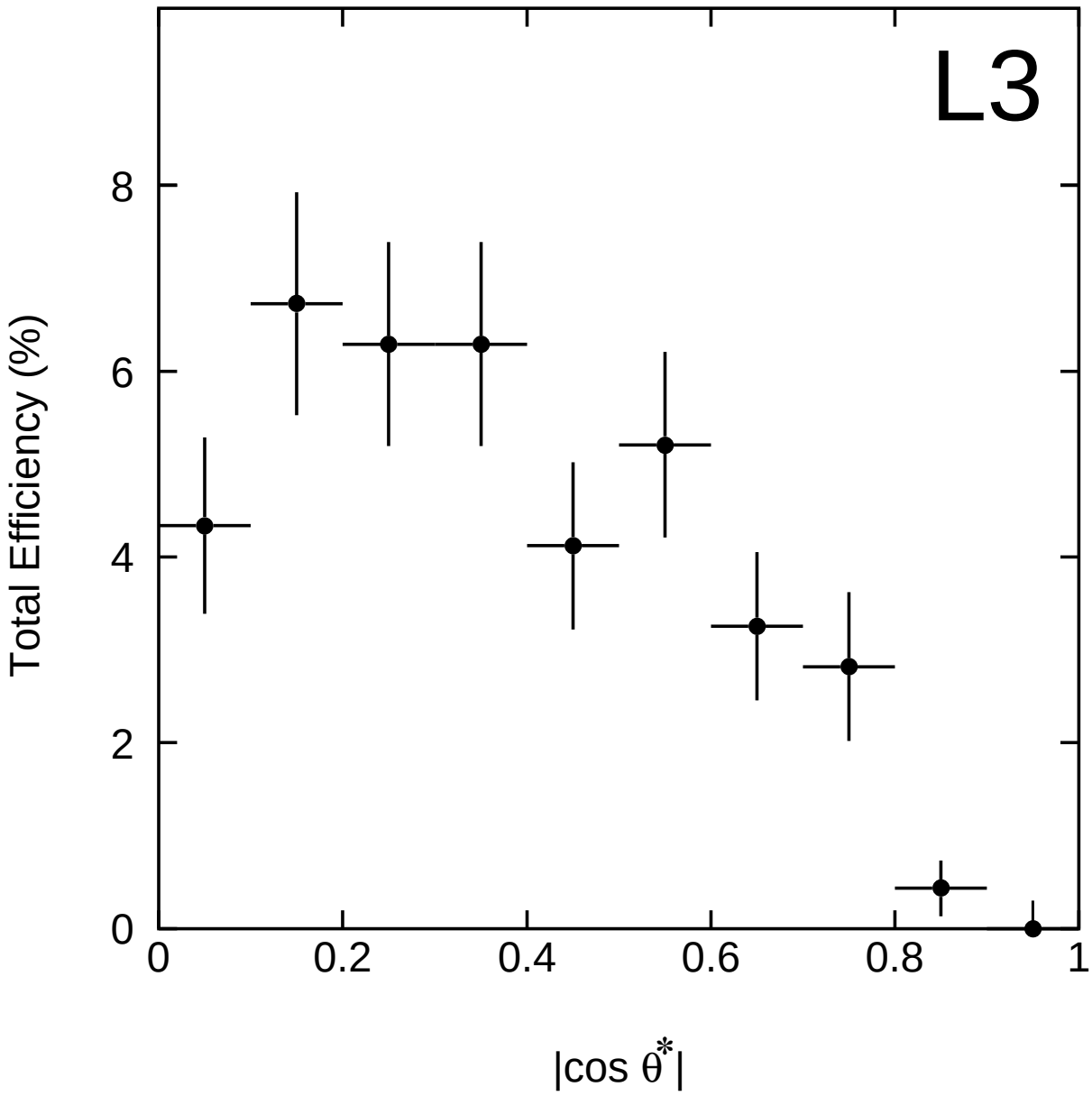

Figure 3

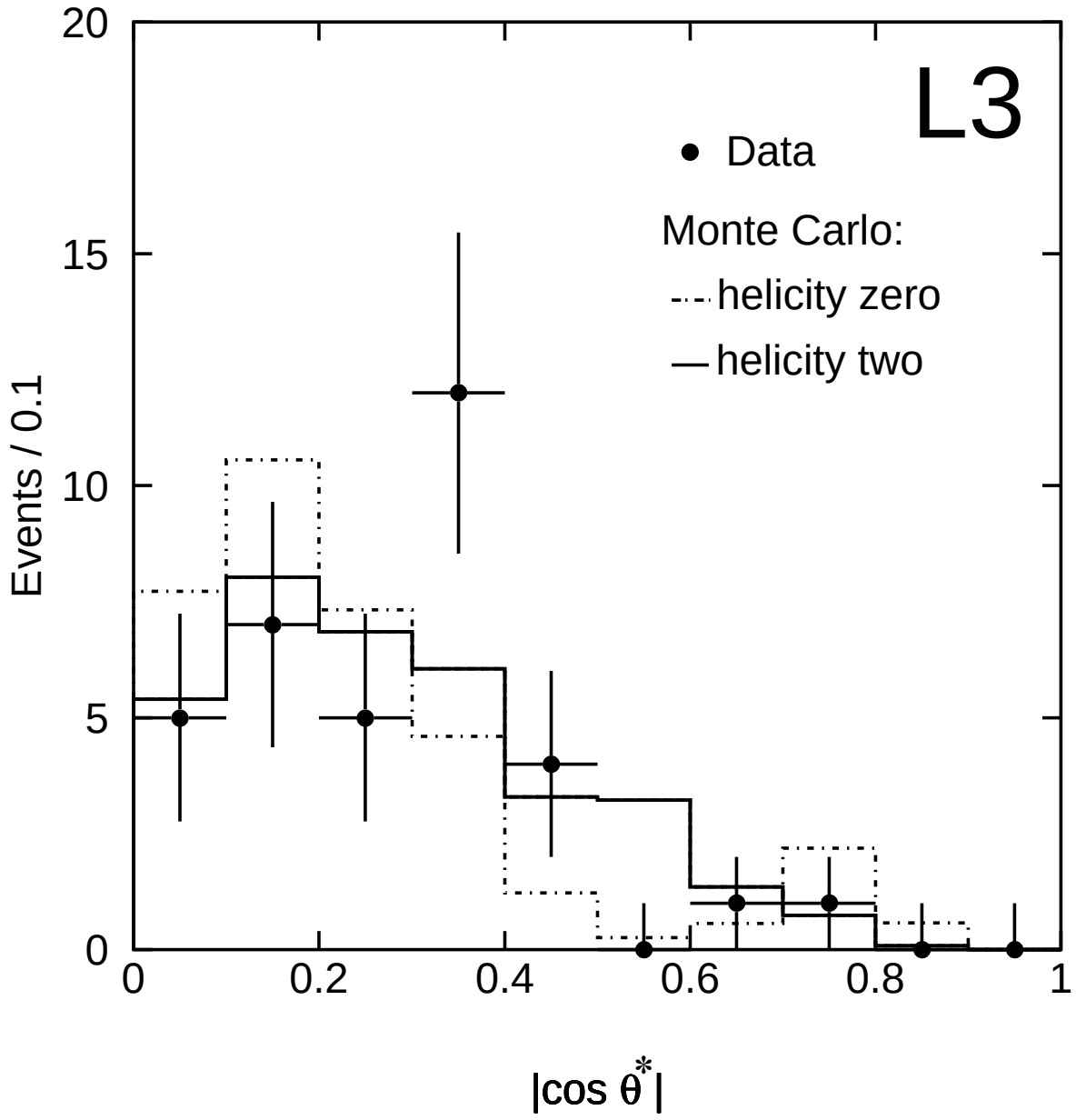
L3
Data
Monte Carlo:
helicity zero
helicity two
Events / 0.1
|cos θ*|
0
5
10
15
20
0
0.2
0.4
0.6
0.8
1

Figure 4